

Effect of cryorolling on the microstructure and mechanical properties of AA2198 alloy

B. Srinivasarao¹, W. Lefebvre¹

¹Groupe de physique des Matériaux, CNRS – UMR 6634, St. Etienne du Rouvray, France

Aluminum alloy (AA2198) was subjected to rolling up to 84% thickness reduction at liquid nitrogen temperature. The hardness values after solid solution treatment, cryorolling and subsequent aging at 135°C for 30h are 78, 152 and 199 Hv respectively. Solid solution treatment and artificial aging at 150°C for 4 days give rise to 165 Hv, indicating that with cryorolling treatment increased peak hardness values are obtained at lower aging temperature and reduced aging time. Transmission electron microscopy reveals that the microstructure after cryorolling consists of elongated dislocation cells with dense dislocation wall structures suggesting that the faster precipitation kinetics is the result of high dislocation density. After the peak aging treatment, the dislocation density was decreased and a high density of nanoscale precipitates was observed resulting in high peak hardness. The precipitates predominantly consists of T_1 (Al_2CuLi) and θ' (Al_2Cu) phases.

Keywords: Cryorolling, Ultrafine grained microstructure, Aging, Precipitation, aluminum alloys.

1. Introduction

Ultrafine-grained and nanocrystalline materials gained a significant interest recently, because of their good mechanical and physical properties [1-4]. Even though these materials exhibit excellent strength values their lack of sufficient ductility limits their use in structural applications. Several strategies have been proposed to overcome this difficulty and one of the most popular methods to obtain a balance between strength and ductility is to develop a microstructure containing ultrafine grain size with a dispersion of nano-precipitate particles in it [5-7]. This microstructure is obtained by a two step process. Initially, the material is subjected to heavy deformation to produce an ultrafine grained structure and suitable heat treatment was selected to create a uniform dispersion of nano-precipitates [8]. Among the several deformation methods, cryorolling technique (CR) has been used to produce ultrafine grain size in several materials for e.g., Al, Al2219, Al7075, Cu and V [9-13]. In this process firstly, the temperature of the material is lowered to liquid nitrogen temperature by immersing in liquid nitrogen then it is subjected to rolling treatment to achieve a total thickness reduction > 80%. To achieve this thickness reduction several passes are necessary and after every pass the material is immersed back in the liquid nitrogen for a sufficient time to lower its temperature. This process presents several advantages. First, ultrafine dislocation cell structure or grains are created after CR. Second, super saturated solid solution is preserved even after deformation. Third, a huge defect density is created which in turn leads to increased number of potential nucleation sites during further heat treatment. Finally, in some cases the un-dissolved precipitates during solid solution treatment could be dissolved during CR [9,10]. Suitable heat treatment temperature will be applied to these CR samples to form nano precipitates which will increase strength and in some instances increase both strength and ductility simultaneously [10].

Al-Cu-Li alloys are most widely used as aerospace materials due to their low density, good specific strength and fracture toughness values [14, 15]. The strength of these alloys could be further improved by either reducing the grain size and/or by increasing the precipitate density. This can be achieved by subjecting these alloys to CR and subsequent heat treatment. Therefore the objective of this paper is to study the effect of CR and subsequent thermal treatment on the microstructure and mechanical properties of model Al2198 alloy.

2. Experimental procedure

A 6.1 mm thick 2198 alloy plate was provided by Alcan-CRV in T351 condition. The chemical composition is given in Table 1. Several samples (6.1 mm thick x 6.5 mm width x 20 mm length) were cut and sealed in a quartz tube under Ar atmosphere. These samples were solution treated at 540°C for 40 min and quenched in water. Two initial conditions were chosen for the CR process:

SS : Solid solution treated

SA : Solid solution treatment + Aging at 150°C for 16h

It is expected that the precipitates in SA samples will act as effective barriers to dislocations during CR process and refine the microstructure significantly. Prior to CR treatment, the specimens were dipped in liquid nitrogen for 5 min. The total thickness reduction of 84% was achieved in multiple passes with about 5% reduction per pass. After each pass the plate was immersed in liquid nitrogen for 2 min before the next rolling pass. Aging treatments were done on the CR samples at 135, 125 and 115°C and Vickers hardness was measured using 100 gf with a dwell time of 15 sec to observe the general trend of the hardness change. Tensile testing samples were cut using an electric discharge machine and polished into dog bone shaped specimens with a gauge length of 10 mm and a cross-section of 2 mm x 0.8 mm. Uniaxial tensile tests were performed at room temperature using INSTRON 4483 tensile testing machine with a load cell of 2kN and at a crosshead velocity of 0.5 mm/min. Three specimens were used to obtain consistent stress-strain curves. Specimens for transmission electron microscopy (TEM) were punched mechanically, ground to a thickness of 100 μm and twin-jet electropolished in a solution of 1:2 vol. pct. nitric acid : methanol at -20°C. The observation is carried out in a JEOL 2000 FX II microscope operating at 200kV.

Table 1. Composition of AA2198 alloy given in wt%.

AA2198	Cu	Li	Mg	Ag	Zr	Al
Min	2.9	0.8	0.25	0.1	0.04	bal.
Max	3.5	1.1	0.8	0.5	0.08	bal.

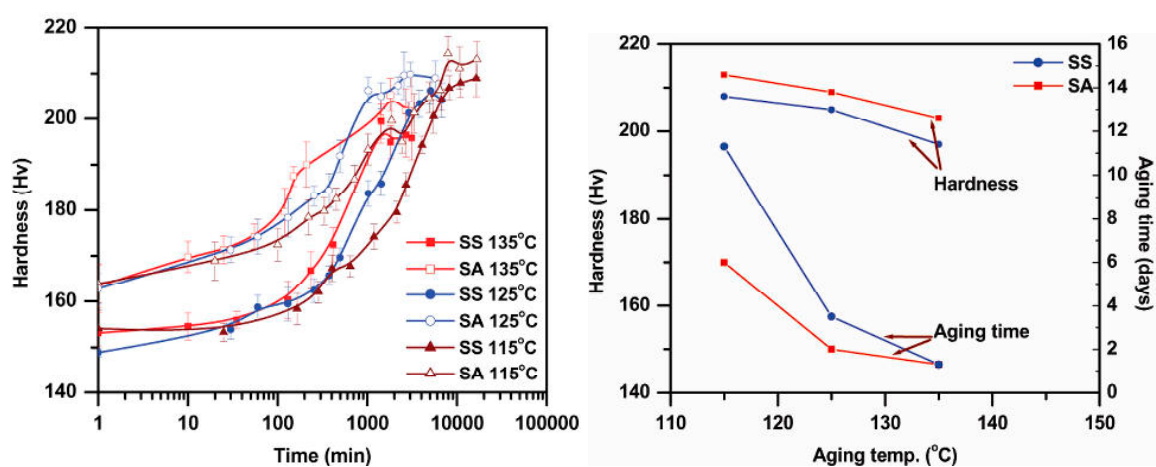


Fig. 1: a) Vickers hardness change during various isothermal aging treatments. All specimens were cryorolled up to 84% thickness reduction. b) Peak hardness and the respective aging time at various isothermal aging temperatures for SS and SA cryorolled samples.

3. Results and Discussion

The hardness values of SS and SA samples before and after CR process are 78, 116, 154 and 162 respectively. Therefore a hardness increase of 50 to 70 Hv could be achieved by CR process alone. Such an increase has also been observed in other alloys for e.g., AA2219 and AA6061 [9, 16]. Hardness variation with aging time at 135, 125 and 115°C is shown in Fig. 1a and 1b shows the peak hardness values and peak aging time with respect to aging time for both SS and SA samples. As the aging temperature decreases both the peak hardness and the time to reach the peak hardness increase analog to conventional aging treatment. The time to reach peak hardness values is much lower and the peak hardness is higher in the case of SA+CR samples than SS+CR samples. This suggests that the SA+CR samples have a higher defect density than SS+CR samples. The defects act as nucleation sites for the precipitation, thereby decreasing the peak aging time and increasing the peak hardness value. The maximum hardness values observed after CR and aging treatments exceed 200 Hv whereas those of the solid solution treated and artificially aged samples show a maximum hardness of only 165 Hv at 150°C for 4 days (figure not shown). CR process is more advantageous than the conventional T6 treatment.

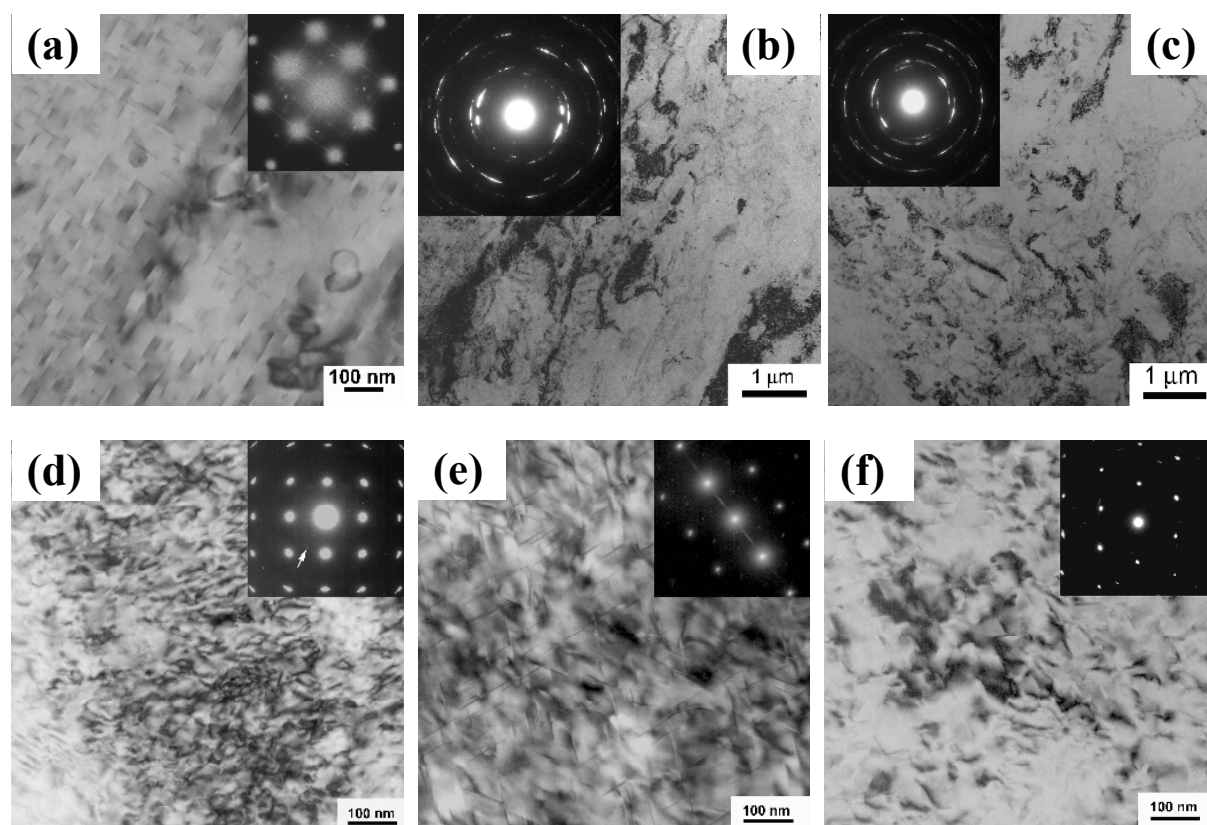


Fig. 2: Bright field TEM micrographs together with their corresponding selected area diffraction pattern. a) SA sample before CR process b) SS sample after CR process c) SA sample after CR process d) High magnification view of SA sample after CR process e) SS sample CR processed and peak aged at 115°C and f) SA sample CR processed and peak aged at 115°C

Fig. 2a shows the TEM micrograph of SA sample. After a short aging treatment at 150°C for 16 h precipitates consists of mostly θ' -Al₂Cu and minor T₁ (Al₂CuLi) and Al₃Zr particles. The presence of these precipitates could be observed from the bright field (BF) image and from the selected area diffraction (SAD) pattern as shown in the inset of Fig. 2a. It has been reported earlier that solid

solution treated Al-Cu-Li alloys contain GP zones, subsequent artificial or natural aging treatment will most likely result in the nucleation of θ' -Al₂Cu whereas solid solution + short stretching dissolves these GP zones and less likely to form θ' phase in the subsequent aging treatment [17, 18]. Fig. 2b and 2c displays typical bright field TEM micrographs of SS+CR and SA+CR samples respectively. These micrographs consist of sub micrometer dislocation cell structures with small orientation difference between them. The presence of θ' precipitates in the SA sample could effectively block the movement of dislocations during CR process and retain high number density which can be observed from Fig. 2d. Even though some of the θ' particles could be seen in Fig. 2d, it is expected that due to intensive dislocation cutting some of them will be dissolved back into the matrix and if there are any GP zones present they will also be dissolved. This could be the reason why the SAD pattern shown in Fig. 2d does not reveal as many spots as the SAD pattern of Fig. 2a i.e., compared with the initial state. Similar strategy has been applied to Al2024 alloy by Cheng et al., where some shear resistant T-phase particles were deliberately left after solid solution treatment [19]. These remnant T-phase particles effectively trapped the dislocations at the interface, increased their density and the microstructure was refined substantially. On further aging treatment this high dislocation density leads to the precipitation of a high density nano-sized S'-phase precipitates. In another study by Shanmugasundaram et al., the undissolved precipitates after solid solution treatment were dissolved into the matrix by CR process [9]. Therefore the faster kinetics of SA samples after CR process could be the result of higher dislocation density. Further evidence could be observed from the TEM micrographs of SS+CR and SA+CR samples after peak aging treatment at 115°C (Fig. 2e and 2f). The precipitates observed are mostly T₁-phase. The T₁ precipitates are much smaller in the case of SA+CR samples than SS+CR samples which is a direct result of the higher nucleation density.

Tensile tests were carried out on three SA+CR samples after peak age hardening at 115°C and Fig. 3 shows the engineering stress-strain curves for this condition. The elastic region part of the curve was removed and only the plastic region was shown in the figure. The samples show yield strength of 550 MPa, ultimate tensile strength of 600 MPa and the plasticity is nearly 8%. The yield strength reported for the original alloy in T851 condition is 430 MPa [20]. Therefore it is possible to improve the strength of the Al2198 alloy by CR and subsequent aging treatment.

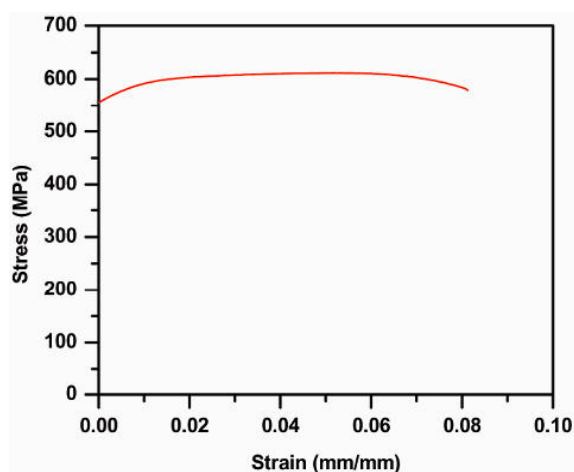


Fig. 3: Engineering stress-strain curves of SA+CR samples heat treated at 115°C for 5 days.

4. Conclusions

Cryorolling and subsequent aging treatments were carried out on Al2198 alloy with two initial conditions. The CR process resulted in very high dislocation density and sub-micrometer elongated dislocation cell structure. The presence of high defect density enhanced the kinetics of the

precipitation process which facilitates the reduction of the aging temperature to less than 135°C whereas conventional T8 aging treatment is carried out at temperatures > 150°C. Retaining a small volume fraction of precipitates before the CR process enhances the defect density and increases the kinetics thereby reducing the peak aging time and increasing the peak hardness value. Good tensile properties such as high yield strength of 550 MPa, ultimate tensile strength of 600 MPa and plasticity of 8 % can be achieved.

Acknowledgements

The authors are grateful to Dr. Alan Guillet (INSA, Rouen) for his assistance in the experiments and discussion. This work has been funded by the ANR and performed in the framework of the research program CONTRAPRECI.

References

- [1] K.S. Kumar, H. Van Swagenhoven and S. Suresh: *Acta Mater.* 51 (2003) 5743.
- [2] H. Gleiter, J. Weissmüller, O. Wollersheim and R. Würschum: *Acta Mater.* 49 (2001) 737.
- [3] O. Gutfleisch, A. Bollero, A. Handstein, D. Hinz, A. Kirchner, A. Yan, K.-H. Müller and L. Schultz: *J. Magnetism and Magnetic Materials* 242-245 (2002) 1277.
- [4] M. Dao, L. Lu, R.J. Asaro, J.T.M. De Hosson and E. Ma: *Acta Mater.* 51 (2007) 4041.
- [5] E. Ma: *JOM* 58 (2006) 49.
- [6] T.S. Wang, Z. Li, B. Zhang, J.M. Deng and F.C. Zhang: *Mater. Sci. Engg. A* 527 (2010) 2798.
- [7] B. Srinivasarao, K. Oh-ishi, T. Ohkubo and K. Hono: *Acta Mater.* 57 (2009) 3529.
- [8] J.K. Kim, H.K. Kim, J.W. Park and W.J. Kim: *Scr. Mater.* 53 (2005) 1207.
- [9] T. Shanmugasundaram, B.S. Murty and V. Subramanya Sarma: *Scr. Mater.* 54 (2006) 2013.
- [10] Y.H. Zhao, X.Z. Liao, S. Cheng, E. Ma and Y.T. Zhu: *Adv. Mater.* 18 (2006) 2280.
- [11] N. Rangaraju, T. Raghuram, B.V. Krishna, K. Prasad Rao and P. Venugopal: *Mater. Sci. Engg. A* 398 (2005) 246.
- [12] Y.B. Chun, S.H. Ahn, D.H. Shin and S.K. Hwang: *Mater. Sci. Engg. A* 508 (2009) 253.
- [13] Y. Wang, M. Chen, F. Zhou and E. Ma: *Nature* 419 (2002) 912.
- [14] S.V. Nair, J.K. Tien and R.C. Bates: *Int. Met. Rev.* 30 (1985) 275.
- [15] N. Eswara Prasad, A.A. Gokhale and P. Rama Rao: *Sadhana* 28 (2003) 209.
- [16] V.L. Niranjani, K.C.H. Kumar and V.S. Sarma: *Mater. Sci. Engg. A* 515 (2009) 169.
- [17] K.S. Kumar, S.A. Brown and J.R. Pickens: *Acta Mater.* 44 (1996) 1899.
- [18] S.P. Ringer, B.C. Muddle and I.J. Polmear: *Meta. Mater. Trans. A* 26 (1995) 1659.
- [19] S. Cheng, Y.H. Zhao, Y.T. Zhu and E. Ma: *Acta Mater.* 55 (2007) 5822.
- [20] P. Cavaliere, M. Cabibbo, F. Panella and A. Squillace: *Materials & Design* 30 (2009) 3622.